

# Thermal imaging-based identification of facial features in noisy environment

Palak Mahajan<sup>1</sup>, Pawanesh Abrol<sup>2</sup>, Parveen Kumar Lehana<sup>3</sup>

<sup>1</sup>Department of Computer Science and Engineering, Central University of Jammu, Jammu and Kashmir (J&K), India

<sup>2</sup>Department of Computer Science and IT, University of Jammu, Jammu and Kashmir (J&K), India

<sup>3</sup>Department of Electronics, University of Jammu, Jammu and Kashmir (J&K), India

## Article Info

### Article history:

Received Jan 16, 2024

Revised May 15, 2024

Accepted Jun 18, 2024

### Keywords:

Feature extraction

Gaussian noise

Salt and pepper noise

Thermal imaging

## ABSTRACT

Face identification is amongst the most efficacious and extensive applications in biometrics involving extraction and locating facial features. With identification being monotonous task attributable to reliance on parameters like varied cameras, fluctuating backgrounds, and exposure to the environment in which an individual is present. Thermal imaging is endeavoring to resolve the accuracy issue of apparent imaging, such as lighting and brightness intensity, among all biometric variables. This paper presents a study of thermal imaging and effective methods involved in the feature extraction process for facial features with thermal imaging under the influence of varied noise. A novel face dataset is created TID comprising 27 thermal images and its corresponding visual band image using Fluke 480 Ti Pro camera. The study analyses detection efficiency of six feature extraction techniques in visible and thermal bands in facial features identification. Also, the influence of noise in the thermal band within the region of interest using feature points  $F_{IN}$ ,  $F_{OUT}$  has been estimated. Throughout TID dataset, ORB extraction technique has been able to identify strongest inlier features  $F_{IN}$  to a maximum extent with detection around the nose, eyes, and mouth. Further, results indicate feature detection in thermal images being invariant to effect of noise for detecting facial features.

This is an open access article under the [CC BY-SA](https://creativecommons.org/licenses/by-sa/4.0/) license.



## Corresponding Author:

Palak Mahajan

Department of Computer Science and Engineering, Central University of Jammu

Jammu and Kashmir (J&K), India

Email: palak.cse@cuammu.ac.in

## 1. INTRODUCTION

An emergent area of computer vision is face recognition, more explicitly face detection in thermal images. The image acquisition process comprises capturing images from a camera. These images can be captured in various wavelengths using different cameras. The images captured in the visible band known as visual images can be captured by optical cameras, while their thermal component can further be captured by infrared cameras. Special infrared vision devices are used to capture the heat emitted by these objects to produce a thermal image. Thermal imaging can be defined as the acquisition of electromagnetic energy generated or reflected by an object in the infrared band of the electromagnetic spectrum [1]. Extracting and detecting facial characteristics in visible band imagery is the most effective method for face recognition. However, face recognition in the thermal spectrum provides significant advantages over face recognition in the visible spectrum. Recent developments in technology, the availability of affordable sensors, and a variety of uses for such imagery, have increased interest in thermal imaging such as in monitoring and surveillance systems. Most of the work done in image processing has been done in the visible spectrum of the image [2].

However, the visible spectrum may not perform well in poor illumination situations or environmental conditions like fog and haze [3]. For face recognition applications, low illumination hinders the performance of the visible spectrum, thereby preventing it from functioning as intended. Thermal imaging whereas is less susceptible to illumination changes hence, the variation in facial features identification due to changes in lighting is less noticeable in thermal images. Infrared radiation is emitted by every object. The radiation is sensed as heat in the far infrared region. Living creatures like humans and animals in general emit more infrared radiation than their surroundings. The thermal infrared (IR) sensor monitors the heat energy emitted by the face instead of detecting reflected light. The heat patterns released by an object serve as the basis for thermal imaging. Depending on their heat and composition, various quantities of IR radiation are emitted by objects. Thermal cameras can capture images in complete darkness and are resistant to changes in illumination, making them suitable for research activities such as night vision surveillance systems [4] and biometrics [5].

Researchers have explored thermal imaging for numerous applications [6]. A YOLOv5 based face detection framework has been proposed by using thermal faces in the wild (TFW) thermal dataset under controlled and uncontrolled environmental factors. The model applied ShuffleNetv2 as its backbone convolutional neural networks (CNN) with pre-trained weights. The model showcased a tradeoff between speed and accuracy while considering vivid image resolutions [7]. Martinez *et al.* [8], a method for automatically identifying eyes and nostrils in face thermal images using Haar and the Gentle Boost algorithm has been demonstrated. The thermal facial characteristics were located using the Harris interest point detector [9]. The Harris interest point algorithm relies on intensity. It uses grey values to identify the existence of an interesting point. Even when the lighting, rotation, and scaling were changed, the experiment still resulted in a large number of interesting points. Based on visible and thermal infrared data, the researcher [10] presented a detailed performance evaluation of different appearance-based face recognition algorithms. They compared algorithms both within the same imaging modality as well as across them. The findings show that employing thermal infrared imagery produces better results in many cases, but performance in both modalities is comparable in others. When visible and thermal infrared pictures are merged, performance improves even further. It also offered a partial explanation for the numerous contradictory statements about the effectiveness of various algorithms on accessible data sets. Guzman *et al.* [11], applying Gabor filters on images of different sizes and orientations expanded face authentication. By dividing the images into tiny modules that localize facial changes, the variations in the faces have been discovered. The behavior of traditional feature point descriptors in images from the long-wave infrared spectral region is evaluated in [12], and the results are compared to those obtained in the visible spectrum. A state-of-the-art methodology is used to assess robustness to changes in scaling, noise, blur, and rotation. In another work [13], a Harris operator-based interest point detector for 3D objects have been introduced, which has been successfully used in computer vision applications. An adaptive technique for determining a vertex's neighborhood has been presented, which is then used to calculate the Harris response for that vertex. The technique was shown to be resistant to a variety of changes, as is evident from the high repeatability values obtained with the SHREC feature detection and description benchmark. Furthermore, Harris 3D surpasses contemporary effective techniques such as heat kernel signatures, according to researchers.

Imaging features produced by a thermal sensor indicate the thermal properties of the facial pattern. Extracting contours in thermal images is an issue that emerges due to the heterogeneous view of the absence of defined boundaries in images. In addition, the majority of the images contain less significant image features, particularly around the eyes and mouth area. In this paper, the analysis for investigating the identification capability of various feature detection techniques has been carried out to detect facial feature points such as eyes, nose, and mouth in varied noise conditions. The influence of two types of noise: Gaussian noise [14] and salt and pepper noise [15] have been analyzed in thermal images. Adding Gaussian noise in the images changes the value of the pixel by averaging the values of its surrounding pixels. The Gaussian noise is represented as the (1) for  $\sigma$  representing the noise factor and  $e$  denoting the Euler number with  $(x, y)$  symbolizing horizontal and vertical distance concerning the center pixel [16].

$$G(x, y) = \frac{1}{2\pi\sigma^2} e^{-(x^2+y^2)/2\sigma^2} \quad (1)$$

The salt and pepper noise (Luo *et al.* [17]) can be represented by (2) given as:

$$n(s) = \begin{cases} N_a, & s = a \\ N_b, & s = b \\ 0, & \text{otherwise} \end{cases} \quad (2)$$

where the intensit of a noisy image's pixels is represented by  $s$ . Additionally,  $a$  and  $b$  stand for noise impulses for dark and light points; when  $b > a$ .

In this work, the thermal images in the infrared band have been explored for the face recognition process. A new face dataset has been created, comprising 27 thermal images along with their corresponding visual band images. For the identification, six feature extraction techniques: features from accelerated segment test (FAST) [18], histogram of oriented gradients (HOG) [19], oriented FAST and rotated BRIEF (ORB) [20], maximally stable extremal regions (MSER) [21], Harris [22], and Eigen [23] have been applied. Table 1 represents a brief description of these feature extraction techniques for computer vision tasks. A comparison has been done to analyze the performance of the feature detection technique in the thermal and visible bands. Also, their efficiency has further been substantiated in detecting facial features in the presence of external noise. The key contributions of this manuscript are as follows:

- A novel face dataset TID is created comprising of thermal images and their corresponding visual band images under different environmental factors.
- The study analyses the detection efficiency of feature extraction techniques in visible and thermal bands.
- The assessment and analysis of noise impact: gaussian and salt and pepper noise in the thermal band within the area of interest have been conducted using feature points.
- Moreover, using the dimensionality reduction technique principal components analysis (PCA), the feature space is optimized by considering the relevant features.

The outline of this work is structured as follows. In section 2, thermal dataset construction has been explained and the overview of the proposed framework is discussed. The analysis and outcomes of the experiments are discussed in section 3. Lastly, the conclusion is presented in section 4.

Table 1. Feature extraction techniques

Techniques	Objective	Summary	Strength	Limitation
FAST	Feature matching feature tracking	Recognizes corners by contrasting pixel brightness	Efficient computation robust to noise	Noise sensitivity low performance with change in lighting
MSER	Region-based object detection image segmentation	Locates areas with consistent intensity fluctuations across varied zoom levels.	Robust to geometric transformations	Sensitive to region size
Harris corner detection	Feature matching feature tracking	Applies eigenvalues to detect corners and calculate the change in intensity for minor window shifts.	Robust to lighting change	Low performance with changes in rotation and scale sensitive to noise
Eigen faces	Face recognition feature extraction	Illustrate faces as linear combinations of images obtained using PCA	Optimize facial feature representation	Sensitive to change in lighting and pose
HOG	Object detection image segmentation	Extracts localized shape information by applying gradient orientations	Captures edge and shape Robust to lighting change	Low performance in a change of scale sensitive to occlusion
ORB	Feature description feature detection feature matching	Integrates FAST keypoint detector with the BRIEF descriptor to incorporate rotational invariance	Efficient computation robust to lighting change	Low performance in the change of scale sensitive to noise

## 2. RESEARCH METHOD

The face dataset has been created at Department of Computer Science and IT and Department of Electronics, University of Jammu, J&K, India. Thermal images have been captured using a Fluke 480 Ti Pro Infrared Camera [24], along with the corresponding visual images. Under varied constraints, images have been collected in pairs, one thermal and one visible. Figure 1 shows the experimental configuration of the image capture process. As illustrated in Figure 1(a), the camera settings have been adjusted for capturing the images. The camera has been placed around 60 cm away from the participants, and with the face at the center of the image. The images have been captured with subjects sitting on chairs at a distance of about 2 feet from the cameras [25]. The rainbow mode is employed for thermal imaging with the image output containing both thermal and RGB images. The images generated by the camera have been saved in JPEG format.

The Fluke 480 stands as a portable infrared thermal camera, the specifications of the camera used are given in Table 2. The images have been captured at a constant temperature of around 27.5°C. The capturing process has been carried out for two consecutive days to maintain the temperature. Different image mode options in Fluke 480 Ti Pro can be employed. Fluke 480 Ti Pro image characteristics have been divided into seven modes: rainbow, ironbow, blue-red, high contrast, amber, hot metal, and grayscale. The color palette processing, display markers adjustment, emissivity settings, and various pre-processing operations on the images captured by the camera have been done using FLUKE SmartView version 4.3.311.0 software. Color palette Ironbow and Grayscale have been a general-purpose palette that instantly detects thermal anomalies and body heat. Rainbow has the optimum color palette for situations with little heat shift and a focus on an area with similar heat intensity. In a broader sense, the face temperature does not change

drastically. The objective is to observe temperature fluctuations in various areas of the face and then employ them for identification purposes. As a result, because the temperature shift is subtle, Rainbow mode has been well suited for face thermal imaging in this study as shown in Figure 1(b).

A sample of the thermal images captured along with their respective visible spectrum images is shown in Figure 2. The raw images obtained of size 1,080×1,440 have been resized to 480×480, for performing image processing operations for better presentation. The camera has been calibrated by first adjusting the temperature between 15 °C and 40 °C, followed by subsequent adjusting of the multipoint focus. The camera generates a pair of both thermal images and visible spectrum images. It examines the raw image and removes sensor noise. Pre-processing techniques like pallet and emissivity have been then employed on processed thermal images to accustom the image accordingly. The emissivity parameter which is the ratio of an object's actual emittance to the emittance of a black body at the same temperature has been set between 0.6 and 1.0. For the sake of uniformity, the emissivity parameters have been set to 0.8. Emissivity is material-dependent and is an important property when measuring temperatures with a thermal camera.

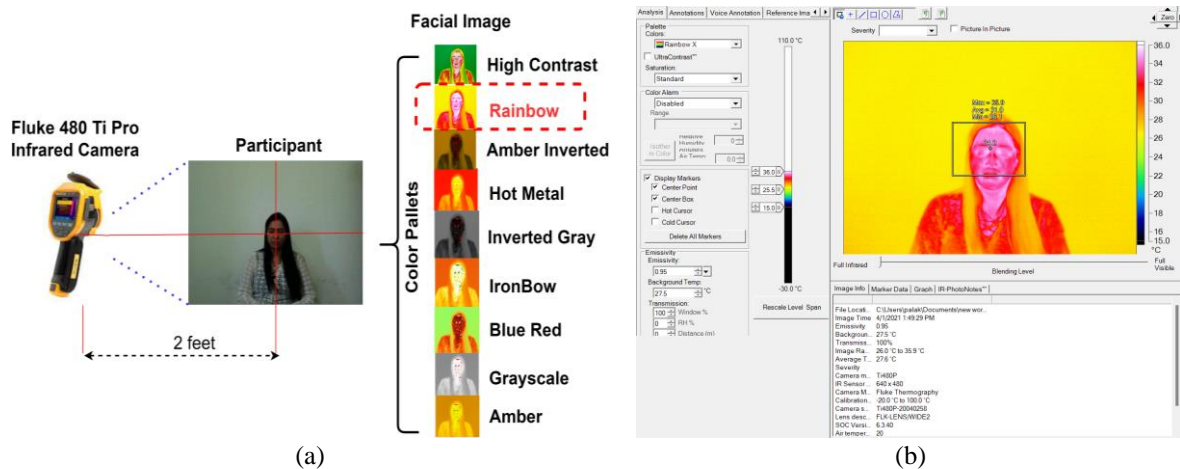


Figure 1. Configuration setting for dataset acquisition (a) illustrated (b) temperature fluctuations

Table 2. Specification table for fluke 480 Ti Pro

Features	Specification
Infrared spectral band	7.5 $\mu$ m to 14 $\mu$ m
Thermal image resolution	640×480
Screen resolution	1280×960
Thermal sensitivity	50 mK
Temperature range	-20 °C to +800 °C
Color pallets	Rainbow, ironbow, blue-red, high contrast, amber, hot metal, grayscale



Figure 2. Thermal and corresponding visual images from the TID dataset

The image has been transformed to greyscale so that feature extraction techniques could perform operations. Further, the thermal images have been enhanced by applying histogram equalization. Data augmentation is additionally done by applying rotation and scaling to increase the size of the dataset.

After generating a grey-level equalized image, external factors noise has been applied to analyze how various feature extraction techniques have been inflated. Figure 3 depicts the framework for assessing the performance of feature descriptors techniques in the infrared band for thermal images. The pseudocode for the proposed methodology is discussed in Algorithm 1. The objective is to discover the sensitivity towards external factors i.e., noise. Two types of noise: Gaussian and salt and pepper noise have been added as noise to the original thermal image. The pixel value has been adjusted by setting the noise density value as 0.01 for salt and pepper noise. Similarly, gaussian noise has been added with mean,  $\mu = 0.1$ .

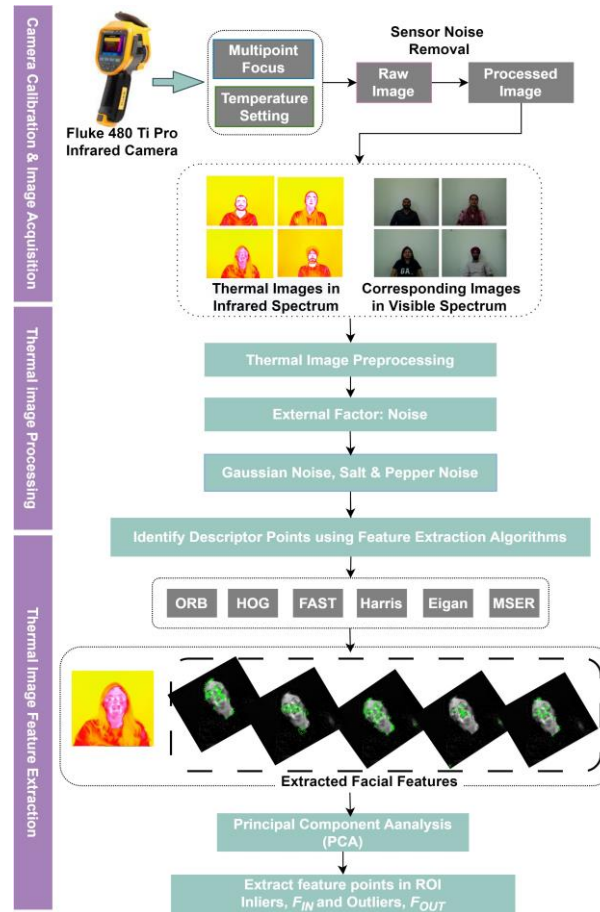


Figure 3. Block diagram of the framework for feature identification in thermal images

#### Algorithm 1. Feature identification in thermal images

**Input:** Thermal image,  $I_{TM}$

**Output:** Feature points: Inliers,  $F_{IN}$  and Outliers,  $F_{OUT}$

**Start**

##### Step I: Calibrate Thermal camera: Radiometric calibration

Set a constant environment with controlled temperature= 27.5°C.  
Warm up the camera for five minutes to attain a steady temperature.  
Use a temperature-controlled blackbody reference source.  
Keep a distance of 2 feet between the subject and the camera.  
Capture the thermal image,  $I_{TM}$ .

##### Step II: Preprocess the thermal image:

for each  $I_{TM} \in \text{TID}$  do  
    Set *color\_pallet*= Rainbow and *emissivity*= 0.8  
    Resize the image = 480x480 resolutions.  
    Convert the image,  $I_{TM}$  into a grayscale image,  $I_{GTM}$   
    Perform histogram equalization on  $I_{GTM}$ , to create enhanced image,  $I_{TEQ}$ .  
    Apply augmentation on  $I_{GTM}$  using rotation= 30° and scaling=0.1  
end for

##### Step III: Introduce External factor noise:

for each image  $I_{TEQ} \in \text{TID}$  do  
    Apply Salt and pepper noise with *noise\_density*=0.01 to create  $I_{TSP}$   
    Additionally, apply Gaussian noise with mean,  $\mu = 0.1$  to create  $I_{TG}$ .  
end for

**Step IV: Extract Thermal Features:**

```

for each image  $I_{TSP}$ ,  $I_{TG} \in$  TID do
    Apply the following feature extraction methods:
        ORB, HOG, FAST, Harris, MSER, Eigen
    Map the identified features for each ROI in every  $I_{TSP}$ , and  $I_{TG}$ .
    Calculate the pertinent thermal features for each ROI.
    Select relevant features around the face by computing feature points:
        Inliers,  $F_{IN}$  and Outliers,  $F_{OUT}$ 
    Further applying PCA to reduce the feature space.
end for

```

A small fraction of noise has been added to the thermal image to study the subtle effect of noise while preserving the thermal properties of the image. The noise value has been selected such that a fine level of distortion is there in the images. Afterward, the feature extraction techniques namely, ORB, FAST, MSER, Harris, HOG, and Eigen functions were applied to the dataset. The features have been extracted thoroughly by each technique. The resultant features are compared and the performance of each feature extractor technique is evaluated. A comparison has also been done between the feature points identified in the images' infrared and visible spectral regions. The sensitivity of these feature extraction techniques toward various factors has been analyzed as well. The evaluation is based on the facial features identified within the inner and outer facial descriptor points.

$$X_p = X * E_K \quad (3)$$

Where  $X_p$  represents the reduced representation of the extracted features for TID dataset for  $X$  image original matrix. The top  $k$  Eigen vectors are represented by  $E_K$  selected from Eigen matrix created using covariance components. Since the size of dataset is small, a minimal value of  $k$  has been selected using hit-and-trial method, specifically  $k = 3$  that converges the data to lower-dimensional space with fast computational speed.

### 3. RESULTS AND DISCUSSION

As discussed above, in this study a Fluke 480 Ti Pro infrared camera has been used to capture the images. The implementation of the algorithm has been done on MATLAB 2019b. The experimental work is performed on Intel(R) Core (TM) i7-8750H CPU with 20 GB RAM accompanied by NVIDIA GeForce GTX 1050Ti. Also for pre-processing the thermal images, the study has employed SmartView software specifically designed for thermal images and compatible with Fluke camera.

#### 3.1. Comparison between visual and infrared spectrum images

As mentioned above, this study investigates the performance of feature identification techniques for detecting facial images in the visible and infrared spectrum that represents spatial and frequency domain respectively. A comparison has been made based on results generated by applying various feature identification techniques. Figure 4 shows the various features extracted by the six feature detection techniques in respective spectrums. The preprocessing done in the visible spectrum is only the color conversion of RGB images into grey-level images. The inlier and outlier features of the facial images have been observed. With inliers being the one that lies completely inside a region of the face and outliers being the one detected outside the facial regions. As can be observed from the images, for visible spectrum images facial features as well as some other features such as text written or texture present in the apparel has also been detected. Almost all feature extraction techniques except ORB have detected only outliers in visible spectrum images as shown in Figure 4(a). On the other hand, in the case of thermal images in the infrared spectrum as illustrated by Figure 4(b), these outlier features have completely been masked and maximum inlier features such as regions near the eyes and cheeks have been observed. With ORB feature extractor identifies the maximum facial features around the inner circle of the face followed by the Harris identifying the inlier features. Overall for almost all 27 images in the TID dataset, HOG identified the least features. Also, it can be therefore concluded that thermal imagery in the infrared spectrum is less sensitive to the variations in exterior features present in the images compared to images in the visible spectrum. Hence for face identification purposes using thermal imaging, the frequency domain performed better in comparison with a spatial domain.

#### 3.2. Identifying the effect of distortions in the infrared spectrum

The investigation entails assessing the thermal image's susceptibility to the noisy environment. Gaussian and salt and pepper noise have been added as noise to the original thermal image. The pixel's value



has been adjusted by setting the noise density value = 0.01 for salt and pepper noise. Similarly, gaussian noise has been added with  $\mu = 0.1$ . A sample of textual facial features identified by various feature extraction techniques under the influence of noise is shown in Figure 5. Here, Figure 5(a) represents the susceptibility of feature extraction methods under salt and pepper noise at noise density value = 0.01 and Figure 5(b) illustrating the effect of gaussian noise (mean = 0.1) on these extraction methods with ORB detecting the maximum features along with the outliers, respectively. Accordingly the computed feature points inliers,  $F_{IN}$ , and outliers,  $F_{OUT}$  for the dataset have been further represented in Table 3 along with their corresponding PCA components. As depicted by the Table 3(a), ORB feature extractor is able to compute maximum number of feature points with  $F_{IN}$  identifying the maximum covered facial region.

For all 27 images in TID, unit variance scaling, and principal components have been calculated using singular value decomposition (SVD) with imputation. In the first two major principal components, PCA account for 81.6% and 7.8% of the total variance, respectively for all six feature detection techniques in the case of inliers as well as outliers. This indicates that PCA effectively condenses the significant information from high-dimensional image component to a smaller set of variable space. This space reduction further accelerates the efficiency of feature detectors by only focusing on most significant features as indicted by Table 3(b), respectively.

Further clustering is performed using correlation distance and average linkage. The output of clustering generates heatmaps for both feature points inliers,  $F_{IN}$ , and outliers,  $F_{OUT}$  is represented in Figure 6, respectively. The heatmap in Figure 6(a) demonstrates high correlation with dark red color representing strong similarity clusters in facial features points with orange colour representing approximately less similarity, and low uncommon distinct features have been illustrated by blue colour. On the otherhand, Figure 6(b) highlights the outlier's heatmap indicating diversions among inconsistent feature points i.e. clusters formed outside facial regions indicated by the colour pallets red, orange, and blue respectively. These heatmap visualization helps in identifying consistant feature point clusters along with illustrating irregularities, thereby enhancing the robustness.

Throughout the entire TID dataset, all six feature detection techniques have been able to identify inlier features to a maximum extent with detection around the nose, eyes, and mouth. With ORB detecting the strongest features amongst the lot. Figure 5 showed external parameters like noise plays a significant role in detecting facial feature in thermal images. Like in the case of Gaussian noise, the noise elements have covered all the regions throughout the image causing the feature extractor to detect more outliers rather than inliers. ORB and MSER, however, show the worst performance in the presence of noise as given in Table 4. Further, as observed from the Figure, feature detection in thermal images is invariant to the effect of noise as the feature extraction techniques were able to detect the facial features.

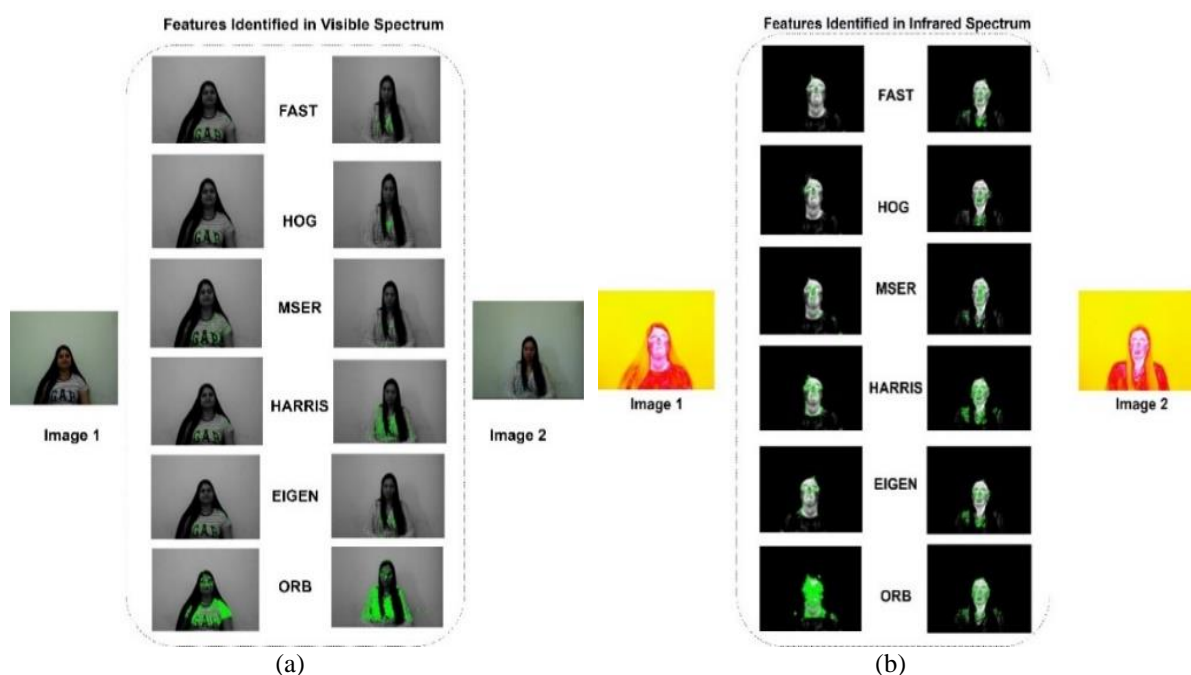


Figure 4. Feature extraction (a) visible spectrum and (b) infrared spectrum

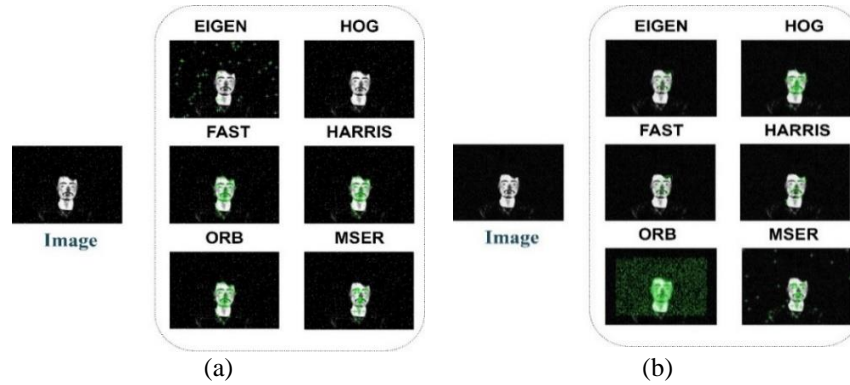


Figure 5. Feature extraction in the presence of (a) salt and pepper noise at noise density=0.01 and (b) gaussian noise at mean=0.1 for the TID dataset

Table 3. Feature extracted within ROI,  $F_{IN}$ , and  $F_{OUT}$ , and their respective PCA components in TID (a)

Image	FAST [18]		Harris [22]		ORB [20]		MSER [21]		HOG [19]		EIGEN [23]	
	$F_{IN}$	$F_{OUT}$	$F_{IN}$	$F_{OUT}$	$F_{IN}$	$F_{OUT}$	$F_{IN}$	$F_{OUT}$	$F_{IN}$	$F_{OUT}$	$F_{IN}$	$F_{OUT}$
I1	49	20	35	15	80	35	53	36	41	6	36	22
I2	55	21	36	14	81	36	69	35	40	14	38	26
I3	62	15	32	18	75	39	60	48	49	12	39	24
I4	43	18	40	20	77	41	62	42	35	7	45	36
I5	45	30	39	22	76	25	63	32	39	12	42	16
I6	52	34	41	25	69	39	71	16	38	15	40	19
I7	69	25	25	7	82	45	55	35	40	9	32	22
I8	75	22	28	19	75	41	54	32	45	7	36	27
I9	31	29	41	18	76	32	56	26	47	8	52	29
I10	52	31	20	12	73	33	66	27	48	8	45	35
I11	56	37	22	14	82	48	62	45	52	9	41	34
I12	51	10	23	9	56	47	60	33	38	16	32	13
I13	49	9	31	13	69	35	58	32	68	20	39	14
I14	60	15	36	15	70	25	59	19	41	5	33	17
I15	59	32	39	22	78	37	55	28	45	8	39	42
I16	58	18	37	21	75	36	45	29	48	7	47	33
I17	69	17	41	25	69	38	58	24	45	5	21	37
I18	45	16	12	35	77	26	62	22	38	13	30	22
I19	44	22	50	14	74	52	57	39	57	11	38	25
I20	42	28	45	19	72	45	58	24	55	15	54	24
I21	48	25	39	22	73	41	71	18	48	17	35	26
I22	50	26	38	26	74	39	66	27	40	7	37	28
I23	55	31	34	14	86	55	65	33	42	4	39	27
I24	56	35	35	7	76	28	62	41	49	15	28	24
I25	54	12	22	16	85	38	68	49	32	10	33	23
I26	53	19	20	18	59	41	59	40	39	11	48	30
I27	55	17	35	22	80	38	60	35	48	14	41	21

PCA components	PC1		PC2		PC3		PC4		PC5		PC6	
	$F_{IN}$	$F_{OUT}$	$F_{IN}$	$F_{OUT}$	$F_{IN}$	$F_{OUT}$	$F_{IN}$	$F_{OUT}$	$F_{IN}$	$F_{OUT}$	$F_{IN}$	$F_{OUT}$
FAST [18]	-0.62	-0.75	-2.89	1.47	0.05	2.40	0.07	-0.35	0.39	0.84	0.00	0.00
Harris [22]	5.34	-2.87	0.49	1.11	-0.55	-2.03	-1.58	0.51	0.22	1.16	0.00	0.00
ORB [20]	-7.39	6.03	1.02	0.51	0.53	-0.82	-0.51	-1.72	0.71	-0.34	-0.00	-0.00
MSER [21]	-2.99	3.20	0.24	-2.82	-1.47	0.33	0.40	1.05	-1.08	0.61	-0.00	-0.00
HOG [19]	1.90	-6.26	0.22	-1.51	1.59	0.03	0.13	-1.14	-1.10	-0.80	-0.00	0.00
EIGEN [23]	3.76	0.65	0.92	1.25	-0.15	0.09	1.49	1.65	0.85	-1.48	-0.00	-0.00

Table 4. Average number of feature points detected

Feature extractor	Inliers	Outliers
FAST [18]	53.22	22.74
Harris [22]	33.18	17.85
ORB [20]	74.78	38.33
MSER [21]	60.52	32.11
HOG [19]	44.70	10.56
EIGEN [23]	38.51	25.78



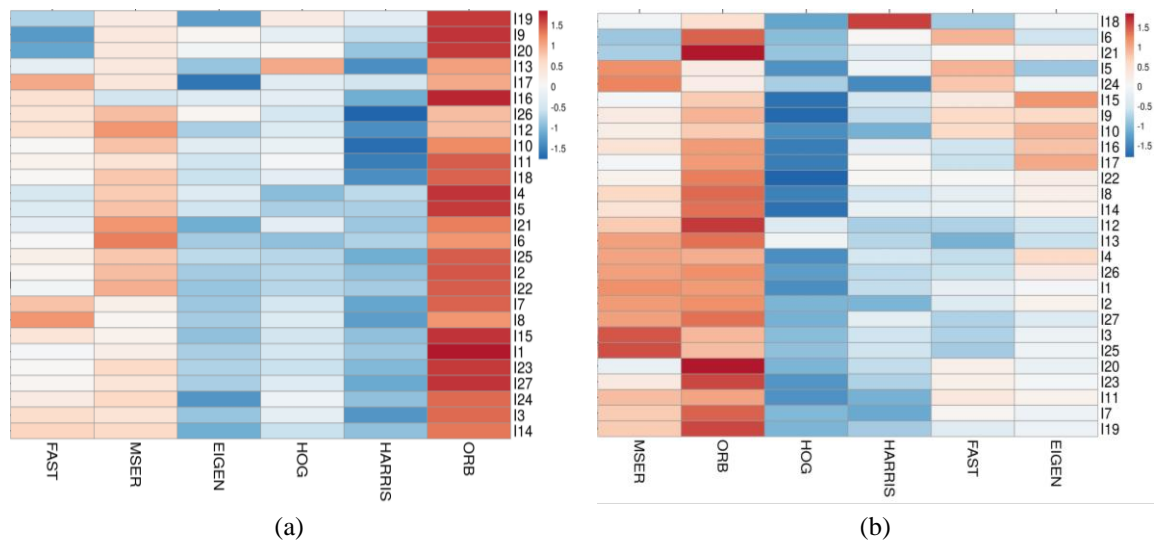


Figure 6. Heatmap showing clusters for various images in the TID dataset for various feature extraction techniques for the dataset (a) inliers heatmap indicating and (b) outliers heatmap indicating

### 3.3. Stastical analysis

As per Table 4, ORB algorithm has detected the strongest and the maximum features for inliers identification, to validate the performance of ORB we can measure the statistical difference between all the algorithms. To test the performance of these feature extraction techniques, let's hypothesized that all algorithms have same performance measure in detecting facial features for thermal images i.e.,  $H_0$ : there is no difference in feature extraction performance of all six algorithms,  $H_1$ : some feature extraction algorithms perform better than the others. Kruskal-Wallis test, a variant of one-way ANOVA test can be considered for measuring the ranking between the algorithms. The feature points outliers, FOUT values predicted by the model have been used in Kruskal-Wallis test to access the ranking of these algorithms. Table 5 represents the performance of feature point detection algorithms using Kruskal-Wallis H test respectively.

Accordingly, Kruskal-Wallis H test indicated that there is a significant difference in the dependent variable between the different groups,  $\chi^2(5) = 103.84$ ,  $p < .001$ , with a mean rank score of 75.63 for FAST, 53.28 for Harris, 135.65 for ORB, 113.54 for MSER, 21.48 for HOG, 89.43 for EIGAN. Further by applying a Bonferroni corrected alpha of 0.0033, the mean ranks of the following pairs are significantly different:  $x_1-x_2$   $x_1-x_3$   $x_1-x_5$   $x_2-x_3$   $x_2-x_4$   $x_3-x_5$   $x_3-x_6$   $x_4-x_5$   $x_4-x_6$  where each  $x_i$  indicates feature extraction algorithm respectively. Since the  $p$ -value  $< \alpha$ ,  $H_0$  is rejected i.e., there is a difference between the mean ranks of some feature extraction algorithms is big enough to be statistically significant as shown by Figure 7. Further,  $p$ -value equals to 0. Hence, we can conclude that the algorithms behave differently with significant performance difference.

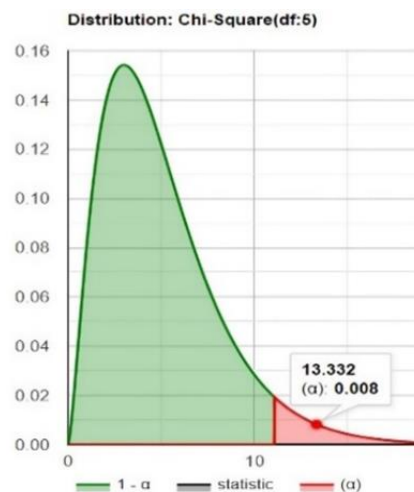


Figure 7. Statistically distributed values for Kruskal-Wallis H test

Table 5. Kruskal-Wallis H test performance for various feature extraction techniques

Group	Harris	ORB	MSER	HOG	EIGAN
FAST	55.7	-58.15	-30.54	49.46	26.63
HarriS	0	-113.85	-86.24	-6.24	-29.07
ORB	-113.85	0	27.61	107.61	84.78
MSER	-86.24	27.61	0	80	57.17
HOG	-6.24	107.61	80	0	-22.83

#### 4. CONCLUSION

Amongst the most popular and effective applications of biometric technology is face recognition. The aspect of thermal images in the infrared band has been explored for the face recognition process. A novel face dataset has been created, comprising 27 thermal images along with their corresponding visual band images. The feature extraction techniques FAST, ORB, MSER, Harris, etc. have been applied for locating facial features like eyes, mouth, and nose. The results showed the sensitivity of visible spectrum images for textural patterns present in the apparel. Almost all techniques except ORB detected only outliers in visible spectrum images. On the other hand, in the case of thermal images in the infrared spectrum, these outlier features have been completely masked, and maximum inlier features such as regions near the eyes and cheeks have been observed. Also, their efficacy has been substantiated in detecting facial features in the presence of external noise. The results showed that external noise plays a significant role in detecting facial features in thermal images. Salt and pepper noise shows less sensitivity as compared to Gaussian noise, as more outliers than inliers have been detected for images with Gaussian noise. Further, the work can be extended by integrating GANs and RNNs to synthesize and augment thermal and visual spectrum images for extensive feature extraction and identification process.





#### REFERENCES

- [1] G. Tanda, "The use of infrared thermography to detect the skin temperature response to physical activity," *Journal of Physics: Conference Series*, vol. 655, no. 1, p. 012062, Nov. 2015, doi: 10.1088/1742-6596/655/1/012062.
- [2] P. Mahajan, P. Abrol, and P. K. Lehana, "Scene based classification of aerial images using convolution neural networks," *Journal of Scientific & Industrial Research*, vol. 79, no. 12, pp. 1087–1094, Dec. 2020, doi: 10.56042/jsir.v79i12.36671.
- [3] P. Mahajan, V. Jakhetiya, P. Abrol, P. K. Lehana, B. N. Subudhi, and S. C. Guntuku, "Perceptual quality evaluation of hazy natural images," *IEEE Transactions on Industrial Informatics*, vol. 17, no. 12, pp. 8046–8056, Dec. 2021, doi: 10.1109/TII.2021.3065439.
- [4] D. Ghose, S. M. Desai, S. Bhattacharya, D. Chakraborty, M. Fiterau, and T. Rahman, "Pedestrian detection in thermal images using saliency maps," *IEEE Computer Society Conference on Computer Vision and Pattern Recognition Workshops*, vol. 2019-June, pp. 988–997, 2019, doi: 10.1109/CVPRW.2019.00130.
- [5] M. K. Bhowmik *et al.*, "Thermal infrared face recognition – a biometric identification technique for robust security system," in *Reviews, Refinements and New Ideas in Face Recognition*, InTech, 2011.
- [6] D. A. Socolinsky, A. Selinger, and J. D. Neuheisel, "Face recognition with visible and thermal infrared imagery," *Computer Vision and Image Understanding*, vol. 91, no. 1–2, pp. 72–114, Jul. 2003, doi: 10.1016/S1077-3142(03)00075-4.
- [7] A. Kuzdeuov, D. Aubakirova, D. Koishigarina, and H. A. Varol, "TFW: annotated thermal faces in the wild dataset," *IEEE Transactions on Information Forensics and Security*, vol. 17, pp. 2084–2094, 2022, doi: 10.1109/TIFS.2022.3177949.
- [8] B. Martinez, X. Binefa, and M. Pantic, "Facial component detection in thermal imagery," in *2010 IEEE Computer Society Conference on Computer Vision and Pattern Recognition - Workshops*, Jun. 2010, pp. 48–54, doi: 10.1109/CVPRW.2010.5543605.
- [9] M. K. Bhowmik, S. Shil, and P. Saha, "Feature points extraction of thermal face using Harris interest point detection," *Procedia Technology*, vol. 10, pp. 724–730, 2013, doi: 10.1016/j.protcy.2013.12.415.
- [10] C. N. Fondje, S. Hu, and B. S. Riggan, "Learning domain and pose invariance for thermal-to-visible face recognition," *IEEE Transactions on Biometrics, Behavior, and Identity Science*, vol. 5, no. 1, pp. 15–28, Jan. 2023, doi: 10.1109/TBIOM.2022.3223055.
- [11] A. M. Guzman *et al.*, "Thermal imaging as a biometrics approach to facial signature authentication," *IEEE Journal of Biomedical and Health Informatics*, vol. 17, no. 1, pp. 214–222, 2013.
- [12] P. Ricaurte, C. Chilán, C. Aguilera-Carrasco, B. Vintimilla, and A. Sappa, "Feature point descriptors: infrared and visible spectra," *Sensors*, vol. 14, no. 2, pp. 3690–3701, Feb. 2014, doi: 10.3390/s140203690.
- [13] I. Sipiran and B. Bustos, "A robust 3D interest points detector based on harris operator," *Eurographics Workshop on 3D Object Retrieval, EG 3DOR*, pp. 7–14, 2010, doi: 10.2312/3DOR/3DOR10/007-014.
- [14] O. Joshua, J. S. Owotogbe, T. S. Ibiyemi, and B. A. Adu, "A comprehensive review on various types of noise in image processing," *International Journal of Scientific and Engineering Research*, vol. 10, pp. 388–393, 2019, [Online]. Available: <http://www.ijser.org>.
- [15] P. B. Dasgupta, "Analytical comparison of noise reduction filters for image restoration using SNR estimation," *International Journal of Computer Trends and Technology*, vol. 17, no. 3, pp. 121–124, Nov. 2014, doi: 10.14445/22312803/IJCTT-V17P123.
- [16] P. Mahajan, P. Abrol, and P. K. Lehana, "Effect of blurring on identification of aerial images using convolution neural networks," in *Lecture Notes in Electrical Engineering*, vol. 597, 2020, pp. 469–484.
- [17] P. Luo, X. Zhang, Z. Chang, and W. Liu, "Research on salt and pepper noise removal method based on adaptive fuzzy median filter," in *2021 IEEE 5th Advanced Information Technology, Electronic and Automation Control Conference (IAEAC)*, Mar. 2021, pp. 387–392, doi: 10.1109/IAEAC50856.2021.9390923.
- [18] E. Rosten and T. Drummond, "Fusing points and lines for high performance tracking," in *Tenth IEEE International Conference on Computer Vision (ICCV'05) Volume 1*, 2005, vol. II, pp. 1508–1515 Vol. 2, doi: 10.1109/ICCV.2005.104.
- [19] N. Dalal and B. Triggs, "Histograms of oriented gradients for human detection," in *2005 IEEE Computer Society Conference on Computer Vision and Pattern Recognition (CVPR '05)*, 2005, vol. 1, no. 7, pp. 886–893, doi: 10.1109/CVPR.2005.177.





- [20] S. A. K. Tareen and Z. Saleem, "A comparative analysis of SIFT, SURF, KAZE, AKAZE, ORB, and BRISK," in *2018 International Conference on Computing, Mathematics and Engineering Technologies (iCoMET)*, Mar. 2018, vol. 2018-Janua, pp. 1–10, doi: 10.1109/ICOMET.2018.8346440.
- [21] D. Nistér and H. Stewénus, "Linear time maximally stable extremal regions," in *Lecture Notes in Computer Science (including subseries Lecture Notes in Artificial Intelligence and Lecture Notes in Bioinformatics)*, vol. 5303 LNCS, no. PART 2, 2008, pp. 183–196.
- [22] C. Harris and M. Stephens, "A combined corner and edge detector," in *Proceedings of the Alvey Vision Conference 1988*, 1988, pp. 23.1–23.6, doi: 10.5244/C.2.23.
- [23] S. Kabi, D. Patra, and G. Panda, "Detection of pneumonia from X-ray images using eigen decomposition and machine learning techniques," in *2022 International Conference on Signal and Information Processing (IConSIP)*, Aug. 2022, pp. 1–5, doi: 10.1109/ICoNSIP49665.2022.10007523.
- [24] FLUKE, "Fluke Ti480 PRO infrared camera," 2024. <https://www.fluke.com/en-us/product/thermal-cameras/ti480-pro> (accessed Oct. 11, 2022).
- [25] M. Kristo, M. Ivasic-Kos, and M. Pobar, "Thermal object detection in difficult weather conditions using YOLO," *IEEE Access*, vol. 8, pp. 125459–125476, 2020, doi: 10.1109/ACCESS.2020.3007481.

## BIOGRAPHIES OF AUTHORS







**Palak Mahajan**     is Assistant Professor at the Department of Computer Science and Engineering, Central University of Jammu, Jammu. She has done his Ph.D. in Computer Science from University of Jammu. She has completed her MTech. in Computer Science Engineering from SMVDU. Dr. Mahajan's research expertise includes artificial intelligence, computer vision and soft computing. She has authored various research articles that have been published in reputed International Journals, Conference Proceedings, and Book Chapters, which are indexed in Web of Science, Scopus, and DBLP. Additionally, she is a member of ACM professional body. She can be contacted at email: palak.cse@cuammu.ac.in.



**Pawanesh Abrol**     is a Professor in the Department of Computer Science and Information Technology, University of Jammu. He holds a Ph.D. in Computer science from the University of Jammu, as well as an MBA (HRM). Dr. Abrol has contributed more than 50 research publications in various reputed national and international proceedings and journals. His research covers aura-based texture analysis, image forgery as well as authentication and eye gaze technologies. He has been the member of various academic bodies such as IETE. He can be contacted at email: pawanesh.abrol@gmail.com.



**Parveen Kumar Lehana**     received the master's degree from Kurukshetra University and the Ph.D. degree in Signal processing from IIT Bombay. He is currently Professor in Department of Electronics at University of Jammu. He has more than 200 research papers in national/international journals to his credit. Also, he has filled several patents and has authored several books. He has given hundreds of invited talks and is life member of several professional bodies, such as IETE, IAPT, and ISTE. He can be contacted at email: pklehana@gmail.com.